ARC Geophysical Research

Higher Temperatures Lead to More Melt-Freeze Crusts in Snowpacks in Cooler Regions of the Pacific Northwest

Clinton D. Alden*[1], Benjamin K. Sullender[2], John Stimberis[3], and Jessica D. Lundquist[1]

[1]Department of Civil and Environmental Engineering, University of Washington
[2]School of Environmental and Forest Sciences, University of Washington
[3]Washington State Department of Transportation

Abstract

Warming winters will lead to a greater fraction of rain falling in traditionally snowy areas. Here we investigate the impact of these changes on snowpack stratigraphy, focusing specifically on the presence and duration of melt-freeze crusts. In this work, we use a hydrologic model with high vertical resolution (Structure for Unifying Multiple Modeling Alternatives, SUMMA) to test the sensitivity of melt-freeze crusts to warming. Model runs with up to 100 layers were initialized with observed precipitation and temperature for 2°C and 4°C uniform warming sensitivity tests. We found warming temperatures increased the frequency of crusts at colder sites, while warmer sites had fewer crusts. Melt-freeze crusts increase the complexity of avalanche forecasting and mitigation for highway, recreational forecasting, and ski area operations. These changes to the snowpack will also impact ecosystem function, with greater snow density altering large mammal movements and predator-prey interactions.

Keywords: Snow Modeling, Wildlife-Snow Interations, Avalanche Forecasting

*Corresponding Author
E-mail address: cdalden@uw.edu
doi:10.5149/ARC-GR.2451

1 Introduction

Warmer winters in the Western United States have led to declines in 1 April snow water equivalent (SWE) [40, 41], reduced days of snow cover [50], and earlier snowmelt timing [1, 2, 36, 42, 53]. However, studies connecting climate warming to snowpack trends have not previously analyzed the layered structure of the snowpack, which has implications for avalanche forecasting [11] and wildlife ecology [54].

To fill an existing literature gap, our work examines the sensitivity of snowpack structure to warming air temperatures. We use observed in situ precipitation and air temperature data at 53 locations in the Pacific Northwest over the past 25 years, combined with uniform temperature increases, to model the detailed layers of the snowpack. We hypothesize that increased temperatures would create a more complex stratigraphy with more ice crusts in maritime snow climates and that near-surface snow density would increase. In this work, changes in stratigraphy refer to changes to the frequency of melt-freeze crusts as defined by Fierz et al. [19] and Greene et al. [22].

Understanding the stratigraphy of a snowpack is critical for avalanche forecasters, and the existence of crusts in a snowpack adds complexity to both forecasting and mitigation operations. Poor snow grain bonding around ice crusts results in unstable snow and avalanches [11]. Additionally, faceted snow grains can develop next to buried crusts and are well known to be a weak interface upon which slab avalanches can be triggered [10, 38, 52].

Melt-freeze crusts from rain-on-snow events also impact wildlife-snow interactions. These layers prevent herbivores, such as reindeer (*Rangifer tarandus*), from digging through the snow to access forage during the winter season, increasing mortality for some species [23]. Melt-freeze crusts also increase the near-surface snow density, which impacts predator-prey interactions in Washington and Alaska [54]. The presence of melt-freeze crusts in a snowpack reduces the snow's insulating properties for species in cold climates with shallow snowpacks [5, 28]. This study builds on prior research examining how warming temperatures and climate variability influence snow stratigraphy in Scandinavia. Vikhamar-Schuler et al. [55] successfully used a multi-layer snow model to reproduce high-density melt-freeze crusts within seasonal snow from significant historical reindeer mortality events in recent decades in Norway. While previous work has explored the sensitivity of stratigraphy to warming temperatures and climate change in that region [45–47], similar questions have yet to be explored in the Western United States. This work in Scandinavia is on predominantly shallow, arctic snowpacks. While arctic snow is generally cold enough to freeze any rain on snow, this may not be true for maritime regions, such as the Pacific Northwest (PNW) of the United States, where snow may be so warm that no refreezing occurs. Therefore, we hypothesize that the impact of warming temperatures on snowpack structure may vary by region.

Here, we conduct a uniform temperature change (ΔT) modeling experiment in the U.S. Pacific Northwest to test the sensitivity of snowpack structure, particularly crust structure, to warming temperatures. Specifically, we investigate (1) how snow stratigraphy, specifically the presence and persistence of melt-freeze crusts, changes with warmer air temperatures, and (2) how these changes vary across geographic and climatic regions. Section 2 describes our methods, Section 3 our results, and we discuss their implications in Section 4 and conclude in Section 5.

2 Methods

2.1 Study Domain

The Natural Resource Conservation Service's SNOwpack TELemetry (SNOTEL) network encompasses 900+ automated surface meteorology and snow study sites across the Western United States [20, 49]. We chose a set of SNOwpack TELemetry (SNOTEL) sites from the Pacific Northwest to the Inland Northwest to the Rockies to compare trends in snow stratigraphy across geographic space and a variety of climatic conditions (Fig. 1). Within this domain, we selected the 53 SNOTEL sites that were both near a ski area and had at least a 25-year period of record (from 2000-2024). The sites range in elevation from 1204m to 2865m elevation and in mean winter (December-January-February) air temperature from $-0.7°C$ to $-8.8°C$. We chose sites located near ski areas to represent where humans travel and live in the winter.

The climatology of our domain is strongly controlled by the Cascade Mountains that run North-South across Central Oregon and Washington (Figure 1). To the west of the Cascade crest, mean winter precipitation is high with mild winter air temperatures due to its proximity to maritime air masses and the ocean [35]. Mean precipitation increases and mean temperatures decrease moving North towards the Washington-Canada border at 49°N, the northern boundary of our domain. East of the Cascades, mean winter precipitation and temperatures decrease (Figure 1).

2.2 Model Choice

For this work, we used the Structure for Unifying Multiple Modeling Alternatives (SUMMA) [8, 9], set up as a variable layer model. Other multi-layer snow modeling options include SNTHERM [27], CROCUS [7], and SNOWPACK [3, 31, 32]. SUMMA allows for the quick modification of parameterizations, including comparing modeling schemes used in separate models run within the same framework. Many previous studies have successfully used the SUMMA modeling framework to represent various snowpack processes. Cristea et al. [13], Currier et al. [14], and Wayand et al. [57] all used SUMMA to model snowpack processes in the Greater Pacific Northwest region. In particular, Cristea et al. (2022) ran SUMMA in the Western United States and in the Alps to effectively evaluate the impact layering schemes had on other snow hydrology processes. SUMMA was run at hourly time steps with a high vertical resolution, allowing for the representation of small layers and interfaces that cannot be resolved with more vertically coarse modeling systems. We chose SUMMA for this work over other high-resolution models for its ease of use in tuning parameterizations, ensuring certain snow properties, such as stratigraphy, were properly resolved.

The SUMMA configuration used a layering scheme described by Jordan [27] with up to 100 layers ranging in thickness between 1cm and 5cm. Each timestep is split into two sequential steps using an implicit Euler time approximation scheme [9]. First, the processes that affect layer thickness are calculated, including precipitation fluxes, snow compaction, and sublimation. Then, thermodynamic and hydrologic fluxes are calculated, including radiative fluxes and phase changes. At the end of each timestep, the layers are subdivided if any have a thickness greater than 5cm or combined if any have a thickness less than 1cm. Layers are only created and destroyed at the top of the snowpack, which maintains layers throughout the accumulation season and represents melt-freeze crusts well. To accurately represent crust formation in physics-based snow models, previous work by Wever et al. [58] highlights the need to solve the Richards' equation. SUMMA uses the Richards' equation to solve for liquid water flow through snow [9], which is the process we are trying to resolve here in investigating ice crusts formed by rain on snow. Each layer has individual properties such as temperature, density, and thickness that were extracted at each timestep for further analysis.

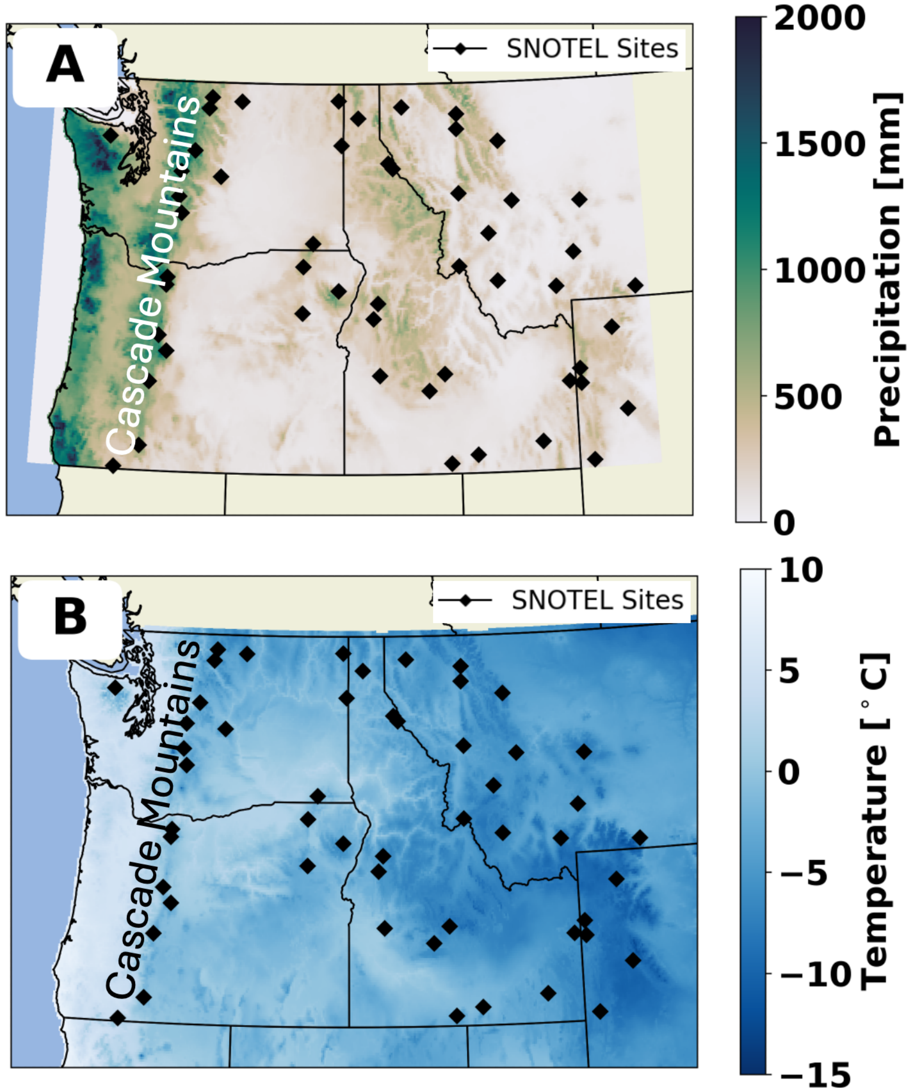

Figure 1: (A) 1991-2020 mean winter (December-January-February) precipitation for our domain from the Parameter Regression against Independent Slopes Model (PRISM) at 4km resolution [16]. (B) PRISM 4km 1991-2020 mean winter air temperature. Black diamonds represent selected SNOTEL sites.

2.3 Experiment Design

To create a representative range of current snow structure conditions, we ran SUMMA for the 2000-2024 period, generating the mean annual statistics for each site, as described in subsection 3.2. Climate models simulate mean annual warming in the Pacific Northwest ranging from 1.8°C to 6.1°C over the 2071-2099 period, compared to 1971-1999 [15]. We tested the sensitivity of snowpack stratigraphy to temperature change (ΔT) by simulating uniform warming of 2°C and 4°C.

2.4 Meteorological Forcings

SUMMA requires input of air temperature, precipitation, incoming longwave radiation, incoming shortwave radiation, wind speed, specific humidity, and air pressure. We used observed air temperature and precipitation at hourly timesteps from the SNOTEL network. The remaining five meteorological inputs used empirical derivations because the SNOTEL network did not contain this data. Table 1 details these data sources, and subsection A.2 provides the derivations.

The ΔT model runs tested two incremental warming scenarios by uniformly increasing air temperature by 2°C and 4°C at all timesteps. We recalculated incoming longwave radiation for each set of model forcings using the modified temperatures (Table 1). The other five meteorological inputs remained unchanged compared to the original model.

Table 1: Meteorological forcings from SUMMA simulations

Forcing Variable	**Temp. Eval.** *Kettle Ponds, CO*	**Density Eval.** *Snoqualmie Pass, WA*	**SNOTEL Sensitivities**
Precip. rate ($kg\,m^2\,s^{-1}$)	observed	observed	observed
Air temperature (K)	observed	observed	observed
Specific humidity ($g\,g^{-1}$)	observed	Running et al. [48]	Running et al. [48]
Wind speed ($m\,s^{-1}$)	observed	uniform 2 $m\ s^{-1}$	uniform 2 $m\ s^{-1}$
Air pressure (Pa)	observed	Wallace and Hobbs [56]	Wallace and Hobbs [56]
Shortwave rad. ($W\ m^{-2}$)	observed	Bennett et al. [4]	Bennett et al. [4]
Longwave rad. ($W\ m^{-2}$)	observed	Dilley and O'Brien [17]	Dilley and O'Brien [17]

2.5 Evaluation Methods

We evaluated our SUMMA simulations to test the representation of internal physical snow processes, specifically temperature and stratigraphy. We evaluated stratigraphy at Snoqualmie Pass, Washington using manual daily snow pit observations collected by the Washington State Department of Transportation (WSDOT). Evaluating for dates with a crust vs. without, we created a binary data set from both model output and snow pit observations for 1 December to 31 March for Water Years (WYs) 2014-2016 and 2018-2024. Snow pit observations from WY 2017 were missing from the WSDOT dataset. WSDOT's Snoqualmie Pass site is unique in the Western US for detailed, consistent, and archived manual snow pit observations near a high-quality weather station.

At Snoqualmie Pass, snow temperatures were almost always near freezing. Therefore, we evaluated SUMMA's internal temperature configuration against vertical snow temperature profile data from the Kettle Ponds site near Crested Butte, Colorado from the Sublimation of Snow campaign [33]. This field campaign deployed this instrument during Water Year 2023. Using this high-quality temperature data from a buried thermistor array, we tuned the model parameters to best represent the vertical profile of internal snow temperature. The temperature array had thermistors every 10cm from snow depths of 40cm to 150cm above the soil. The Kettle Ponds simulations used observed meteorological forcing to generate hourly SUMMA output for Winter 2022-2023. Starting with the parameterizations from the Reynolds Mountain, Idaho test case from Clark et al. [9], which included the atmospheric stability scheme from Mahrt and Gamage [34] and the Hedstrom and Pomeroy [25] method to calculate new snow density, we calibrated the thermal conductivity, atmospheric stability, and new snow density parameters by comparing modeled snow temperature to Kettle Ponds observations. We iterated within a range of thermal conductivity values from 0.15 $W\ m^{-1}K^{-1}$ to 0.5 $W\ m^{-1}K^{-1}$ and ultimately selected 0.35 $W\ m^{-1}K^{-1}$. The final selected model set up and parameter values are detailed in Table A1 and Table A2 in the appendix. The rain-snow partitioning temperature was set at 0°C based on the conclusions of Currier et al. [14] using the SUMMA model in Washington State. We found the best fit of parameter values and model schemes using this configuration with a mean internal temperature bias 1.5°C colder than observations at Kettle Ponds.

2.6 Melt-freeze Crust Formation

In this paper, crusts refer specifically to melt-freeze crusts. As defined in Fierz et al. [19] and Greene et al. [22], they are formed by a surface layer of snow ”that refroze after having been wetted by melt or rainfall.” These occur when the temperature oscillates from below to above freezing and back (Figure 2A, observed air temperature at Olallie Meadows, WA). SUMMA runs with these observed temperatures simulated thin layers of high-density snow (Figure 2B). With 2°C warming, this site would not observe sub-freezing temperatures for longer periods of time and would hypothetically have had fewer crusts.

The Olallie Meadows site is the closest SNOTEL to the WSDOT manual snow pit observations at Snoqualmie Pass. Manual snow pits, as shown in Figure 2C, are frequently dug by avalanche forecasters to collect data on the relative hardness of different layers in the snowpack. Vertical hand hardness profiles were one of WSDOT's primary observations collected with snow pits. These hand hardness measurements estimated how resistant a layer is to penetration by a fist (very soft), four fingers (soft), one finger (medium), a pencil (hard), or a knife (very hard). This subjective yet repeatable metric has been widely used in the avalanche industry to identify unique layers in snow pits [19]. For this work, we classified pencil and knife-hard snow in the WSDOT snow pits as crusts. This method identified crusts on 474 days between 1 December and 31 March for WYs 2014-2016 and 2018-2024 (39% of days).

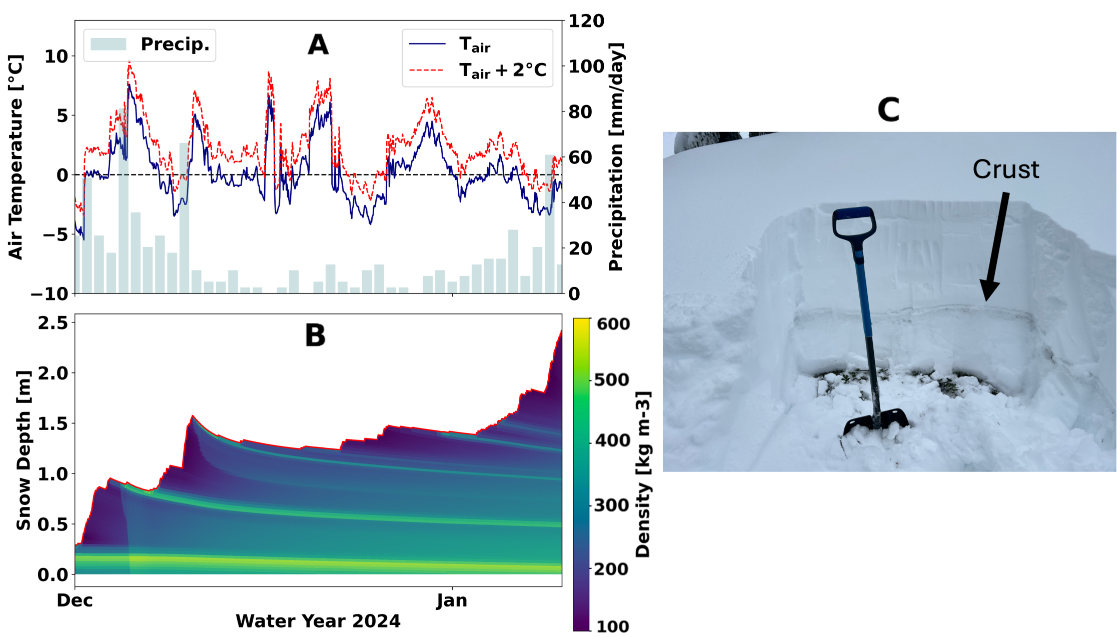

Figure 2: (A) Observed air temperature from the Olallie Meadows SNOTEL site near Snoqualmie Pass, Washington, observed air temperature +2°C, and observed precipitation. (B) SUMMA modeled density and depth using the observed temperature for Ollalie Meadows SNOTEL for 1 December 2023 to 10 January 2024. (C) Example of a crust from a snow pit. Photo credit: Clinton Alden.

2.7 Crust Identification Algorithm

We tested several algorithms to identify crusts in SUMMA output by comparing them against daily snow pit observations from WSDOT at Snoqualmie Pass. With SUMMA output (e.g., Figure 2B), we subdivided the snowpack into overlapping 15cm sections of snow depth centered at 5cm increments. Using the average density of each of these 15cm sections, we identified crusts where any of these sections increased by at least 150 $kg\ m^{-3}$ when compared to the layer below, during times when the average temperature of all layers is less than the melting temperature ($0°C$). The latter filter eliminated the time steps when the snowpack is isothermal in spring. Because of the constant rate compaction scheme used in SUMMA [9], the refreezing of liquid water from either melt or rain-on-snow events was the only physical process that could create a layer with a higher density than the layer below it vertically. As used here, SUMMA is a point model with no horizontal redistribution of snow. The model did not modify snow density as a function of wind speed, and as a result, it did not simulate wind crusts.

Complex mesoscale temperature inversions occur at many passes in the Washington Cascades in the winter, including at Snoqualmie Pass [51, 57]. These cold air pools create difficulty in representing precipitation type correctly. To address this issue, we ran SUMMA simulations from the nearby Olallie Meadows SNOTEL for this crust identification comparison. Rain is regularly observed while the pass level wet-bulb temperatures are below freezing [57]. As such, using meteorological forcing from this site near Snoqualmie Pass but above this shallow cold air pool provides a more realistic representation of the precipitation phase in snow models. This decision was made based on careful analysis of the local meteorology across a number of stations. We created a binary dataset with both observations and model output, denoting days with crusts and without crusts between December 1 and March 31. We did not tune SUMMA to match crusts but instead evaluated its ability to represent crusts in the results (subsection 3.1).

3 Results

3.1 Model Evaluation

Here, we compared SUMMA model output for the Olallie Meadows SNOTEL to manual snowpit observations from the Washington State Department of Transportation snow study site at the nearby Snoqualmie Pass to evaluate the crust algorithm's ability to detect crusts in SUMMA output for Water Years (WYs) 2014-2016 and 2018-2024. Data from WY 2017 for Snoqualmie Pass was missing from the WSDOT dataset. We highlight two dates in WY 2024 with crusts (22 December and 10 February) and one date without crusts in the top 1m (23 January), represented in both manual and modeled snow profiles (Figure 3). On 22 December and 10 February, WSDOT recorded crusts in manual snow pit observations, buried 15cm and 10cm below the top of the snowpack respectively. SUMMA model output and our crust algorithm also identified melt-freeze crusts on these dates at similar depths. On 10 February, no crusts were found in manual in situ observations. Similarly, SUMMA output for this date did not show any high-density layers (crusts) in the top 1m of the snowpack.

Table 2: Crust Detection Model vs Manual Observations - Snoqualmie Pass, Washington - Water Years 2014-2016, 2018-2024

	No Observed Crust	**Observed Crust**
No Modeled Crust	652 (54%) True Negative	233 (19%) False Negative
Modeled Crust	87 (7%) False Positive	241 (20%) True Positive

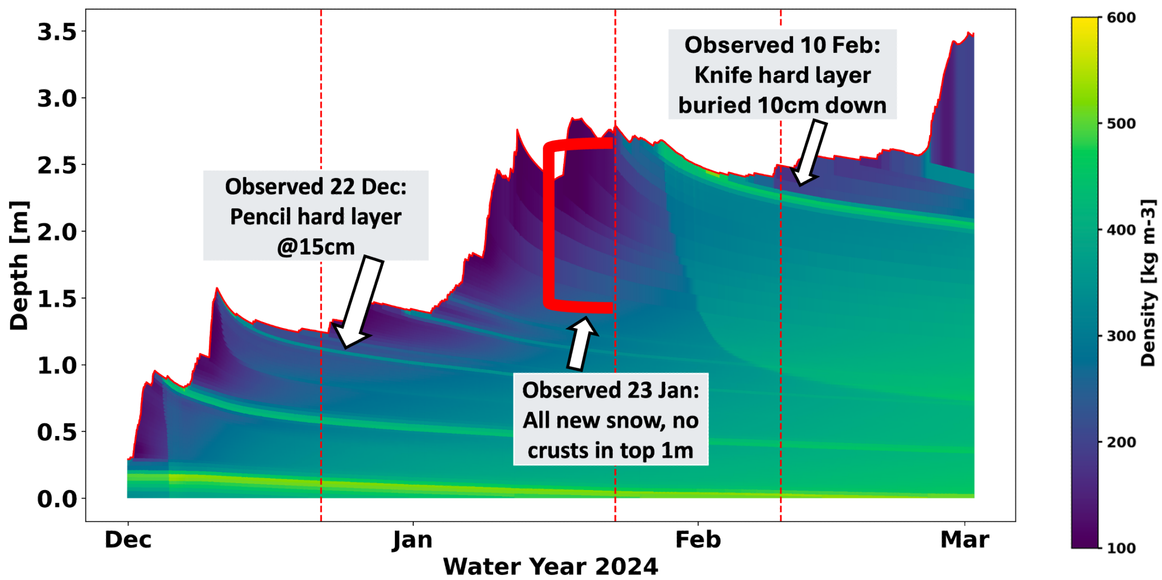

Figure 3: Modeled snow density and depth for Snoqualmie Pass, Washington for 1 December 2023 to 1 March 2024. Manual snow pit hand hardness measurements for the site from the WSDOT are annotated on 22 December, 23 January, and 10 February.

Using the crust identification algorithm discussed in subsection 2.6, our model correctly matched 74% of the observations (Table 2). All modeled years in this dataset matched observations at least 66% of the winter. When observed crust was present, the model correctly identified it 51% of the time. When no crust was observed, the model simulated this correctly 88% of the time. When the model simulated a crust, it was correct 74% of the time. Thus, the model tends to predict crusts less frequently than they are observed in snow pits, but overall provides a more accurate assessment of crust frequency than predicting climatological averages.

3.2 Snowpack Changes

The first of two criteria used to quantify stratigraphy changes was the change in the number of winter days with a crust present (ΔCD) between current climate and warmed model runs. This quantity is defined in Equation 1. CD (crust-days) represents the average number of days with a crust present between 1 December and 31 March for each site.

$$\Delta CD = CD_{warm} - CD_{current} \tag{1}$$

The second criterion was the percent of the snow-covered season with an isothermal snowpack as defined in Equation 2 where ID (isothermal days) represents days where the average snowpack temperature was equal to $0°C$ and SCD represents the average snow-covered days for each site. An isothermal snowpack as calculated here is where the vertically-averaged snow temperature was warmer than $-0.1°C$.

$$\%I = \frac{ID}{SCD} \tag{2}$$

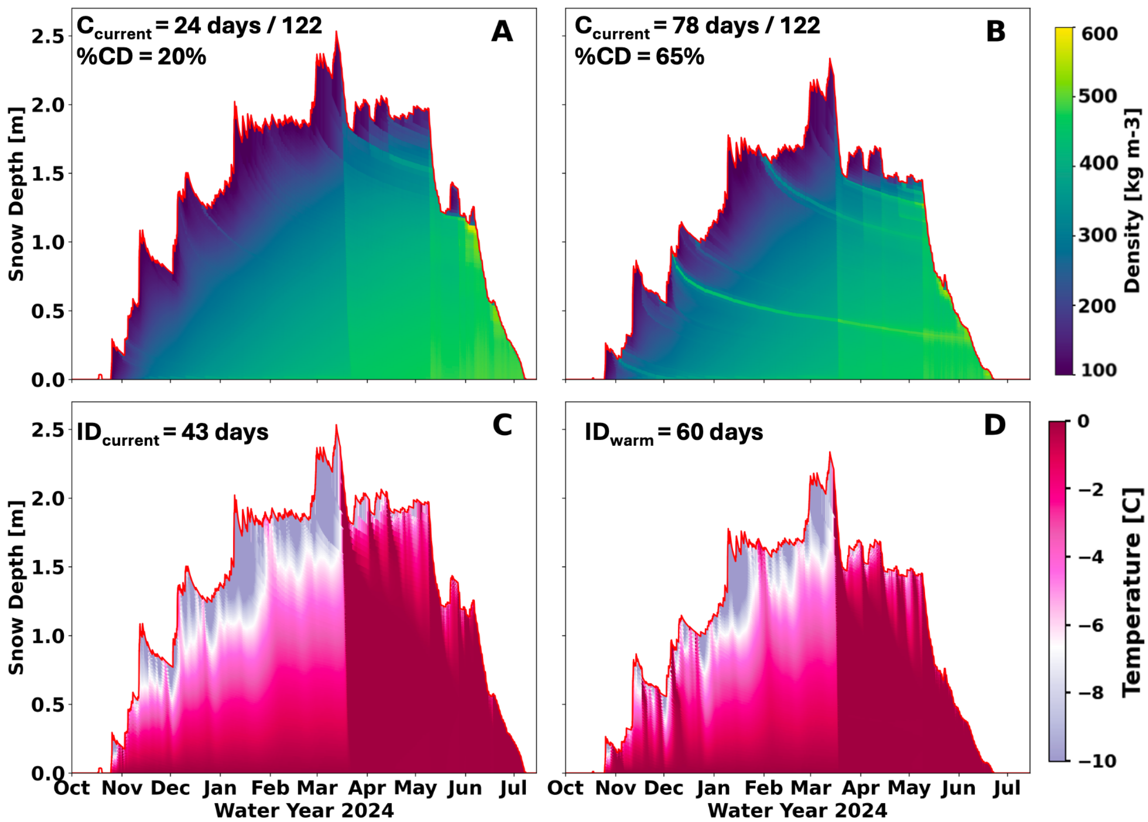

Figure 4: (A) Water year 2024 SUMMA modeled snow depth and density for Harts Pass with observed meteorology. (B) Modeled snow depth and density for the same year at Harts Pass with 2°C of warming. (C) Modeled snow depth and temperatures for Harts Pass initialized with observed meteorology. (D) Modeled snow depth and temperatures for Harts Pass with 2°C of warming.

In general, in the current climate, warmer sites had fewer days with melt-freeze crusts (i.e., western Oregon), while cooler locations had more crust days (i.e., interior Idaho). We compared the number of melt-freeze crusts in both the current climate and warming scenarios and observed trends that varied between the sites. As seen in Figure 5, warmer sites closer to the Pacific Ocean had fewer days with crusts in the +2°C model run. The opposite was true for sites cooler sites and those further inland, where most sites in Idaho, Wyoming, and Montana had more days with crusts with warming.

The change in number of winter days with a crust (ΔCD, see Equation 1 above) was negatively correlated with the mean winter air temperature at any given site (Figure 6). Sites with colder mean December-January-February (DJF) air temperatures saw an increase in crust days with warming, while those with warmer mean winter air temperatures saw fewer days with crusts with warming.

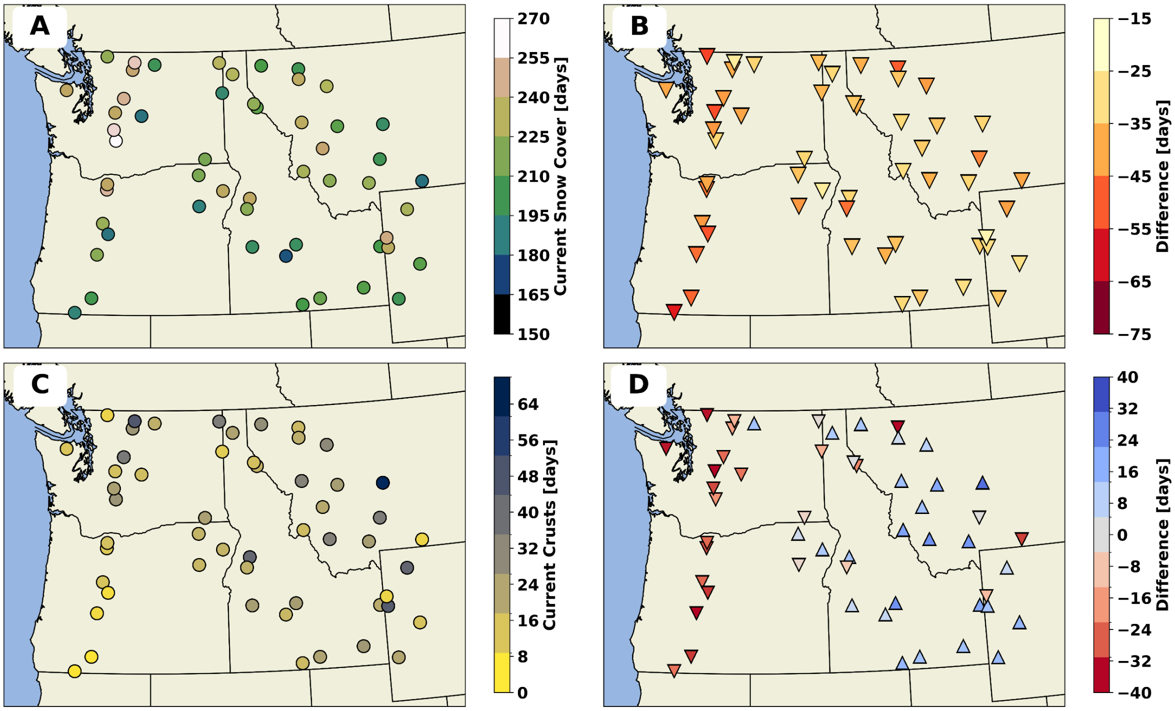

Figure 5: (A) The average number of snow cover days in the current climate model simulations, $SCD_{current}$. (B) The change in the number of snow cover days with 2°C of simulated warming, ΔSCD. (C) The number of days in the current climate model simulations with a crust present, $CD_{current}$. (D) The change in the number of days with a crust with 2°C of simulated warming, ΔCD.

All sites had a higher percentage of the snow season with an isothermal snowpack for both air temperature warming scenarios when compared to the current climate model runs (Figure 6A). Sites with a higher current mean DJF air temperature experienced a higher percent change in isothermal temperatures for both warming scenarios (Figure 6A). The relationship was stronger for the 4°C warming scenario, indicating that with more warming, sites are isothermal for an even greater fraction of the time.

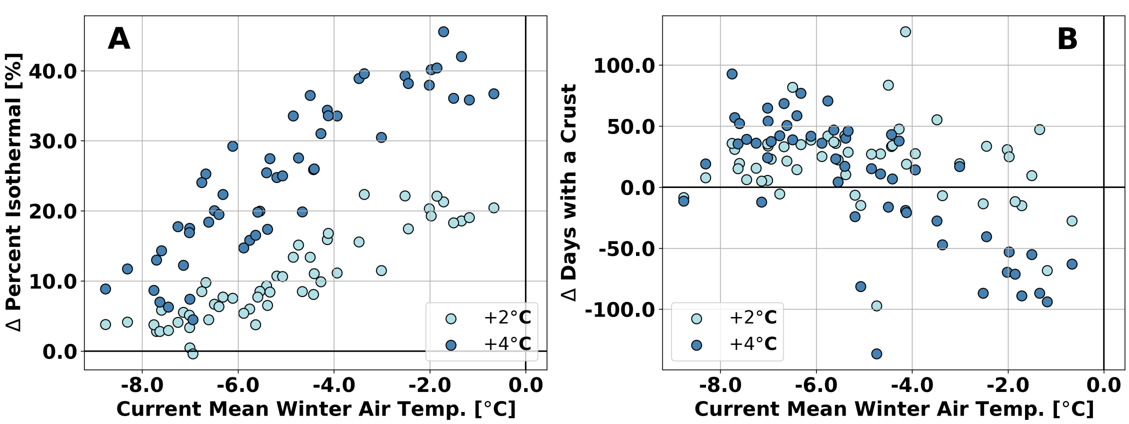

Figure 6: (A) Percent change in days with an isothermal snowpack ($\Delta\%I$) and mean winter air temperature (DJF) for the +2°C and +4°C warming scenarios compared to present. (B) Change in number of days with a crust ΔCD compared to mean winter air temperature (DJF).

4 Discussion

4.1 Stratigraphy Changes

The relationship between the trend in melt-freeze crusts with warming and mean winter air temperature can be explained by the process by which these crusts are formed. Melt-freeze crust formation requires liquid water from either melt or rain-on-snow (RoS) events to be present in a cold snowpack with a vertically-averaged temperature below freezing. With warming, more rain will fall, on average, than in the current climate [26]. In warmer regions, the average snowpack will not be cold enough to freeze liquid water passing through it and thus will not have the distinct melt-freeze crusts in question. If a site is too warm, rain may either fall directly on the ground without snow or fall on a homogeneous snowpack that lacks cold snow. However, in cooler regions, a future warmed climate will still possess cold snow and thus will have more crust days with more frequent RoS events in a warmed climate (ie., Harts Pass, WA, see Figure 4).

The results discussed in subsection 3.2 demonstrate different trends that develop across the Pacific Northwest because crust formation requires rain falling on cold snow. A snowpack with an isothermal temperature profile at 0°C lacks the cold content required to exchange latent heat energy with incoming rain to refreeze. Figure 6 shows that sites with warmer mean winter air temperatures in the current climate have a greater shift towards more days with an isothermal snowpack than colder sites. These warm sites are predominantly in the maritime snow climates of the Cascade Mountains of western Oregon and western Washington. If air temperatures warm, these sites would see even fewer snow-covered days (Figure 5B), fewer mid-winter freezing temperatures, and therefore, fewer crusts (Figure 5D).

4.2 Wildlife Implications

Changing snow stratigraphy and the frequency of ice crusts within seasonal snow also have implications for wildlife. Many large herbivores forage in the winter by digging through the snowpack to reach buried grasses, lichen, and other food sources [18, 43]. Previous research has identified the number of days of the winter with ice present in a snowpack as having a significant negative impact on reindeer (*Rangifer tarandus*) population growth rates [23]. More ice crusts may increase winter mortality rates of herbivores for which winter food availability is already a significant bottleneck [44]. Conversely, increased winter mortality may benefit scavengers such as Arctic foxes (*Vulpes lagopus*) and boost carnivore populations [6, 24].

Changes in stratigraphy may also impact animal movement. While ice crusts can lock up forage for herbivores, increased snow density may improve the movement abilities of some animals. Carnivores, such as wolves, gain an even more pronounced locomotion advantage in denser snow [54], which may be linked with observations of increased predation rates in snowier winters [39].

Given the spatial patterns of our results, the changes to wildlife populations will vary depending on the region. Warmer regions with fewer crusts may enhance forage accessibility and, therefore, benefit herbivore populations. In colder areas, on the other hand, more frequent rain-on-snow events will render forage inaccessible for herbivores. Regardless, the shrinking snow season that we observe across all regions provides a reduced window of opportunity for predators to exploit movement advantages, although greater melt-freeze crusts and increased density may boost hunting effectiveness within these limited times.

4.3 Avalanche Implications

The model simulations show an increase in ice crusts as a result of more frequent winter rain-on-snow events in areas that currently have colder climates. The transition to a higher fraction of wintertime precipitation falling as rain has already begun in the Western United States, particularly in the Pacific Northwest [26, 29].

Changes to melt-freeze crust stratigraphy impact avalanche type, size, frequency, and mitigation practices. With more thick melt-freeze crusts persisting throughout the winter in the snowpack, meltwater can pool on these interfaces, increasing the likelihood of large (scale D2) to very large (D3+) wet slab avalanches [37]. The dynamics of wet slab avalanches are more complex than the typical storm slab and wet loose avalanche problems faced by avalanche mitigation professionals. The presence of ice crusts can also prolong avalanche instability during the spring as meltwater reactivates avalanche activity on a previously dormant melt-freeze crust. In some instances, wet slab avalanches can be nearly impossible to trigger with explosives and require days, if not weeks, for the snowpack to regain strength. For avalanche practitioners, this can complicate mitigation work and delay the opening of seasonal roads and ski terrain. Additionally, crusts provide a smooth and fast bed surface for avalanches to run on. With this bed surface, avalanches can run further and faster down their path.

Stratigraphy changes, such as ice crusts, create vertical discontinuities in the pore space and conductivity between snow grains in different layers. These discontinuities, in turn, create a non-linear temperature profile in snow that is not yet isothermal. Above and below the interfaces between these crusts and other layers, sharp temperature gradients can exist, higher than the $1°C/10$cm threshold needed for kinetic metamorphism, or faceting [37]. Facets are a critical weak layer that can trigger and propagate avalanches, requiring careful consideration for forecasting and mitigation.

As snowpack stratigraphy evolves, avalanche forecasting operations must adapt to a new paradigm. Currently, cooler regions that have not experienced ice crusts are likely to experience ice crusts in a warmer future. Reliance on past experience alone may no longer suffice to guide future decision-making. Heuristics and institutional knowledge about snowpack behavior within an operational boundary become inadequate when faced with the types of changes described in this work. If snow stratigraphy shifts in a specific region, corresponding adjustments to avalanche forecasting and mitigation strategies may be necessary. It will be imperative to transfer knowledge from those who have historically experienced snowpacks with many melt-freeze crusts to forecasting operations in regions that have not.

5 Conclusion

A warming climate has significant impacts on seasonal snow cover. In this study, we modeled the sensitivity of snowpack structure to climate warming across 53 SNOTEL sites in the Pacific Northwest. Using observed precipitation and temperature data from 2000 to 2024, we simulated statistics about snowpack duration, temperature structure, and crust presence/absence for each site under current conditions and with uniform temperature increases of $2°C$ and $4°C$. The results showed that cooler, inland sites experienced more crust formation, while warmer sites in Oregon and Washington exhibited fewer crusts under the modeled warming scenarios. Furthermore, all sites demonstrated an increased percentage of the snow season with an isothermal snowpack at both warming thresholds. In addition to this change in isothermal temperatures, warmer locations lost more days with snow cover than cooler sites.

Crusts introduce new challenges for avalanche forecasting operations. Weak, faceted snow grains can form near buried crusts, potentially altering the type and frequency of avalanches in a region. These findings also have implications for wildlife biology, as crusts affect animals' ability to access buried forage and navigate the winter landscape.

Acknowledgements

We acknowledge funding support from the National Aeronautics and Space Administration (NASA) Interdisciplinary Research in Earth Science program, Grant #80NSSC20K1291. BKS supported by NASA FINESST Award #80NSSC24K1582 and the University of Washington Program on Climate Change's Graubard Fellowship.

Data Availability

SUMMA is an open-source model available at `https://ral.ucar.edu/model/summa`, detailed in Clark et al. [8, 9]. A repository with the code used to run the models and analyze our results is available at `https://github.com/clinton-alden/summa_icelayers/`.

Author Contributions

CDA - Conceptualization, Methodology, Writing-Original Draft, Writing-Review and Editing, Visualization
BKS - Methodology, Writing-Review and Editing
JS - Methodology, Writing-Review and Editing
JDL - Conceptualization, Methodology, Writing-Original Draft, Writing-Review and Editing, Visualization

A Appendix

A.1 Model Decisions and Parameter Choices

Table A1: SUMMA Model Key Parameterization Values

Model Parameter Name	Model Parameter Description	Value
tempCritRain T_{crit} ($°C$)	Rain/snow partitioning temperature	$0°C$
newSnowDenMin	Min Density of New Snow	50 $kg\ m^{-3}$
densScalGrowth	Compaction Rate	0.1
fixedThermalCond_snow	Thermal Conductivity of Snow	0.35
Fcapil	Capillary Pressure	0.04

Table A2: SUMMA Model Key Model Decisions

Model Decision Name	Model Decision Description	Choice
snowLayers	Snow Layering Scheme	jrdn1991
snowDenNew	New Snow Density Scale	hedAndPom
compaction	Compaction Scheme	consettl
astability	Atmospheric Stability	mahrtexp

A.2 Model Forcing Derivations

Due to previously recognized errors with the temperature observations in the SNOTEL network, adjustments to temperature observations were made using the correction discussed in

Currier et al. [14]. This error is a result of an erroneous conversion from voltage to degrees Celsius, resulting in a warm bias at colder temperatures. The temperature correction is as follows:

$$T_{corr} = 1.03 \times T_{SNTL} - 0.90 \tag{3}$$

where T_{corr} is corrected temperature in $°C$ and T_{SNTL} is raw observed temperature in $°C$. This correction methodology from Currier et al. [14] used a least squares regression of temperature observations from secondary instrumentation co-located at SNOTEL sites in Western Washington.

Observations of wind speed, air pressure, specific humidity, incoming shortwave radiation, and incoming longwave radiation are not consistently collected at SNOTEL sites. Therefore, various empirical methods and approximations were employed to fill the meteorological forcing dataset used by SUMMA.

Air pressure was derived using the hypsometric equation with the typical scale height of the atmosphere and standard sea level pressure to determine an average air pressure for the elevation of the site, given by:

$$p_{typical} = p_0 \exp\left(\frac{-z}{H}\right) \tag{4}$$

where $p_{typical}$ is the typical/average air pressure for a given elevation, $p_0 = 101325Pa$ is the standard sea level air pressure, z is the elevation of the site above sea level in meters, and $H = 8000m$ is the scale height of the atmosphere for mid-latitudes. Once typical air pressure is calculated, specific humidity and virtual temperature are calculated for each hourly time step using $p_{typical}$. Air pressure can then be recomputed using the hypsometric equation with virtual temperature for each time step as seen below where $g = 9.8\frac{m}{s^2}$, $R_d = 287\frac{J}{kgK}$, and T_v represents the virtual temperature.

$$p = p_0 \exp\left(\frac{-zg}{R_d T_v}\right) \tag{5}$$

Specific humidity is filled by assuming a running minimum temperature to approximate the dew point using the method described in Running et al. [48]. For each hourly time step, the lowest temperature in the antecedent or subsequent 12 hours (24-hour window) is assumed to be the dew point. From dew point and air temperatures, relative humidity and thus specific humidity can be calculated using the following empirical relationship for each timestep [30]:

$$RH = 100 - 5(T_a - T_d) \tag{6}$$

where T_a and T_d represent air and dewpoint temperatures in $°C$ respectively.

Wind speed was assumed to be $2m/s$ at all time steps, consistent with other studies using uniform wind speed in the absence of quality in situ observations [12].

Incoming shortwave radiation was generated using the MetSim methodology developed by Bennett et al. [4] using latitude, time of day, and time of year to generate theoretical maximum solar insolation values for each time step. A cloud correction was then applied using air temperature and precipitation to approximate cloud albedo.

Incoming longwave radiation was calculated using the empirical relationship from Dilley and O'Brien [17], defined as

$$LW = 59.38 + 113.7\left(\frac{T_a}{273.16}\right)^6 + 96.96\sqrt{\frac{465 \cdot e_0}{2.5 \cdot T_a}} \quad (7)$$

where T_a is air temperature in K and e_0 is vapor pressure in kPa. Currier et al. [14] explored the different empirical longwave radiation schemes described in Flerchinger et al. [21] against observations at Snoqualmie Pass, Washington. They found the Dilley and O'Brien method to be the most accurate, which we used to generate forcing radiative fluxes for our model simulations.

References

[1] N. W. Arnell. The effect of climate change on hydrological regimes in Europe: A continental perspective. *Global Environmental Change*, 9(1):5–23, Apr. 1999. ISSN 0959-3780. doi: 10.1016/S0959-3780(98)00015-6.

[2] T. P. Barnett, J. C. Adam, and D. P. Lettenmaier. Potential impacts of a warming climate on water availability in snow-dominated regions. *Nature*, 438(7066):303–309, Nov. 2005. ISSN 1476-4687. doi: 10.1038/nature04141.

[3] P. Bartelt and M. Lehning. A physical SNOWPACK model for the Swiss avalanche warning: Part I: Numerical model. *Cold Regions Science and Technology*, 35(3):123–145, Nov. 2002. ISSN 0165-232X. doi: 10.1016/S0165-232X(02)00074-5.

[4] A. R. Bennett, J. J. Hamman, and B. Nijssen. MetSim: A Python package for estimation and disaggregation of meteorological data. *Journal of Open Source Software*, 5(47):2042, Mar. 2020. ISSN 2475-9066. doi: 10.21105/joss.02042.

[5] N. T. Boelman, G. E. Liston, E. Gurarie, A. J. H. Meddens, P. J. Mahoney, P. B. Kirchner, G. Bohrer, T. J. Brinkman, C. L. Cosgrove, J. U. H. Eitel, M. Hebblewhite, J. S. Kimball, S. LaPoint, A. W. Nolin, S. H. Pedersen, L. R. Prugh, A. K. Reinking, and L. A. Vierling. Integrating snow science and wildlife ecology in Arctic-boreal North America. *Environmental Research Letters*, 14(1):010401, Jan. 2019. ISSN 1748-9326. doi: 10.1088/1748-9326/aaeec1.

[6] B. L. Borg and D. W. Schirokauer. The Role of Weather and Long-Term Prey Dynamics as Drivers of Wolf Population Dynamics in a Multi-Prey System. *Frontiers in Ecology and Evolution*, 10, Mar. 2022. ISSN 2296-701X. doi: 10.3389/fevo.2022.791161.

[7] E. Brun, E. Martin, V. Simon, C. Gendre, and C. Coleou. An Energy and Mass Model of Snow Cover Suitable for Operational Avalanche Forecasting. *Journal of Glaciology*, 35 (121):333–342, Jan. 1989. ISSN 0022-1430, 1727-5652. doi: 10.3189/S0022143000009254.

[8] M. P. Clark, B. Nijssen, J. D. Lundquist, D. Kavetski, D. E. Rupp, R. A. Woods, J. E. Freer, E. D. Gutmann, A. W. Wood, L. D. Brekke, J. R. Arnold, D. J. Gochis, and R. M. Rasmussen. A unified approach for process-based hydrologic modeling: 1. Modeling concept. *Water Resources Research*, 51(4):2498–2514, 2015. ISSN 1944-7973. doi: 10.1002/2015WR017198.

[9] M. P. Clark, B. Nijssen, J. D. Lundquist, D. Kavetski, D. E. Rupp, R. A. Woods, J. E. Freer, E. D. Gutmann, A. W. Wood, D. J. Gochis, R. M. Rasmussen, D. G.

Tarboton, V. Mahat, G. N. Flerchinger, and D. G. Marks. A unified approach for process-based hydrologic modeling: 2. Model implementation and case studies. *Water Resources Research*, 51(4):2515–2542, 2015. ISSN 1944-7973. doi: 10.1002/2015WR017200.

[10] S. C. Colbeck. A review of the metamorphism and classification of seasonal snow cover, 1986.

[11] S. C. Colbeck and J. B. Jamieson. The formation of faceted layers above crusts. *Cold Regions Science and Technology*, 33(2):247–252, Dec. 2001. ISSN 0165-232X. doi: 10.1016/S0165-232X(01)00045-3.

[12] N. C. Cristea, J. D. Lundquist, S. P. Loheide II, C. S. Lowry, and C. E. Moore. Modelling how vegetation cover affects climate change impacts on streamflow timing and magnitude in the snowmelt-dominated upper Tuolumne Basin, Sierra Nevada. *Hydrological Processes*, 28(12):3896–3918, 2014. ISSN 1099-1085. doi: 10.1002/hyp.9909.

[13] N. C. Cristea, A. Bennett, B. Nijssen, and J. D. Lundquist. When and Where Are Multiple Snow Layers Important for Simulations of Snow Accumulation and Melt? *Water Resources Research*, 58(10):e2020WR028993, 2022. ISSN 1944-7973. doi: 10.1029/2020WR028993.

[14] W. R. Currier, T. Thorson, and J. D. Lundquist. Independent Evaluation of Frozen Precipitation from WRF and PRISM in the Olympic Mountains. Oct. 2017. doi: 10.1175/JHM-D-17-0026.1.

[15] M. Dalton, P. W. Mote, and A. Snover. Northwest Climate Assessment Report. Technical report, 2013.

[16] C. Daly, R. P. Neilson, and D. L. Phillips. A Statistical-Topographic Model for Mapping Climatological Precipitation over Mountainous Terrain. Feb. 1994. ISSN 1520-0450.

[17] A. C. Dilley and D. M. O'Brien. Estimating downward clear sky long-wave irradiance at the surface from screen temperature and precipitable water. *Quarterly Journal of the Royal Meteorological Society*, 124(549):1391–1401, 1998. ISSN 1477-870X. doi: 10.1002/qj.49712454903.

[18] S. G. Fancy and R. G. White. Energy Expenditures by Caribou while Cratering in Snow. *The Journal of Wildlife Management*, 49(4):987–993, 1985. ISSN 0022-541X. doi: 10.2307/3801384.

[19] C. Fierz, R. Armstrong, and Y. Durand. The International classification for seasonal snow on the ground, 2009.

[20] S. W. Fleming, L. Zukiewicz, M. L. Strobel, H. Hofman, and A. G. Goodbody. SNOtel, the Soil Climate Analysis Network, and water supply forecasting at the Natural Resources Conservation Service: Past, present, and future. *JAWRA Journal of the American Water Resources Association*, 59(4):585–599, 2023. ISSN 1752-1688. doi: 10.1111/1752-1688.13104.

[21] G. N. Flerchinger, W. Xaio, D. Marks, T. J. Sauer, and Q. Yu. Comparison of algorithms for incoming atmospheric long-wave radiation. *Water Resources Research*, 45(3), 2009. ISSN 1944-7973. doi: 10.1029/2008WR007394.

[22] E. Greene, K. Birkeland, K. Elder, M. Staples, and Staples. Snow, Weather, and Avalanches: Observational Guidelines for Avalanche Programs in the United States. 2016.

[23] B. B. Hansen, R. Aanes, I. Herfindal, J. Kohler, and B.-E. Sæther. Climate, icing, and wild arctic reindeer: Past relationships and future prospects. *Ecology*, 92(10):1917–1923, 2011. ISSN 1939-9170. doi: 10.1890/11-0095.1.

[24] B. B. Hansen, V. Grøtan, R. Aanes, B.-E. Sæther, A. Stien, E. Fuglei, R. A. Ims, N. G. Yoccoz, and Å. Ø. Pedersen. Climate Events Synchronize the Dynamics of a Resident Vertebrate Community in the High Arctic. *Science*, 339(6117):313–315, Jan. 2013. doi: 10.1126/science.1226766.

[25] N. R. Hedstrom and J. W. Pomeroy. Measurements and modelling of snow interception in the boreal forest. *Hydrological Processes*, 12(10-11):1611–1625, 1998. ISSN 1099-1085. doi: 10.1002/(SICI)1099-1085(199808/09)12:10/11⟨1611::AID-HYP684⟩3.0.CO;2-4.

[26] K. Ikeda, R. Rasmussen, C. Liu, A. Newman, F. Chen, M. Barlage, E. Gutmann, J. Dudhia, A. Dai, C. Luce, and K. Musselman. Snowfall and snowpack in the Western U.S. as captured by convection permitting climate simulations: Current climate and pseudo global warming future climate. *Climate Dynamics*, 57(7):2191–2215, Oct. 2021. ISSN 1432-0894. doi: 10.1007/s00382-021-05805-w.

[27] R. E. Jordan. A One-dimensional temperature model for a snow cover : Technical documentation for SNTHERM.89. Oct. 1991.

[28] K. L. Kausrud, A. Mysterud, H. Steen, J. O. Vik, E. Østbye, B. Cazelles, E. Framstad, A. M. Eikeset, I. Mysterud, T. Solhøy, and N. C. Stenseth. Linking climate change to lemming cycles. *Nature*, 456(7218):93–97, Nov. 2008. ISSN 1476-4687. doi: 10.1038/nature07442.

[29] N. Knowles, M. D. Dettinger, and D. R. Cayan. Trends in Snowfall versus Rainfall in the Western United States. Sept. 2006. doi: 10.1175/JCLI3850.1.

[30] M. G. Lawrence. The Relationship between Relative Humidity and the Dewpoint Temperature in Moist Air: A Simple Conversion and Applications. Feb. 2005. doi: 10.1175/BAMS-86-2-225.

[31] M. Lehning, P. Bartelt, B. Brown, and C. Fierz. A physical SNOWPACK model for the Swiss avalanche warning: Part III: Meteorological forcing, thin layer formation and evaluation. *Cold Regions Science and Technology*, 35(3):169–184, Nov. 2002. ISSN 0165-232X. doi: 10.1016/S0165-232X(02)00072-1.

[32] M. Lehning, P. Bartelt, B. Brown, C. Fierz, and P. Satyawali. A physical SNOWPACK model for the Swiss avalanche warning: Part II. Snow microstructure. *Cold Regions Science and Technology*, 35(3):147–167, Nov. 2002. ISSN 0165-232X. doi: 10.1016/S0165-232X(02)00073-3.

[33] J. D. Lundquist, J. Vano, E. Gutmann, D. Hogan, E. Schwat, M. Haugeneder, E. Mateo, S. Oncley, C. Roden, E. Osenga, and L. Carver. Sublimation of Snow. June 2024. doi: 10.1175/BAMS-D-23-0191.1.

[34] L. Mahrt and N. Gamage. Observations of Turbulence in Stratified Flow. Apr. 1987. ISSN 1520-0469.

[35] C. Mass. *The Weather of the Pacific Northwest*. University of Washington Press, Sept. 2021. ISBN 978-0-295-74845-0.

[36] G. J. McCabe and M. P. Clark. Trends and Variability in Snowmelt Runoff in the Western United States. Aug. 2005. doi: 10.1175/JHM428.1.

[37] D. McClung and P. A. Schaerer. *The Avalanche Handbook*. The Mountaineers Books, 2006. ISBN 978-0-89886-809-8.

[38] D. M. McClung. Use of Expert Knowledge in Avalanche Forecasting . *Defence Science Journal*, 45(2):117, Mar. 1995. ISSN 0011748X.

[39] L. D. Mech, D. W. Smith, K. M. Murphy, and D. R. MacNulty. Winter Severity and Wolf Predation on a Formerly Wolf-Free Elk Herd. *The Journal of Wildlife Management*, 65 (4):998–1003, 2001. ISSN 0022-541X. doi: 10.2307/3803048.

[40] P. W. Mote, A. F. Hamlet, M. P. Clark, and D. P. Lettenmaier. Declining Mountain Snowpack in Western North America. Jan. 2005. doi: 10.1175/BAMS-86-1-39.

[41] P. W. Mote, S. Li, D. P. Lettenmaier, M. Xiao, and R. Engel. Dramatic declines in snowpack in the western US. *npj Climate and Atmospheric Science*, 1(1):1–6, Mar. 2018. ISSN 2397-3722. doi: 10.1038/s41612-018-0012-1.

[42] K. N. Musselman, M. P. Clark, C. Liu, K. Ikeda, and R. Rasmussen. Slower snowmelt in a warmer world. *Nature Climate Change*, 7(3):214–219, Mar. 2017. ISSN 1758-6798. doi: 10.1038/nclimate3225.

[43] W. Peters, M. Hebblewhite, A. Mysterud, D. Eacker, A. J. M. Hewison, J. D. C. Linnell, S. Focardi, F. Urbano, J. De Groeve, B. Gehr, M. Heurich, A. Jarnemo, P. Kjellander, M. Kröschel, N. Morellet, L. Pedrotti, H. Reinecke, R. Sandfort, L. Sönnichsen, P. Sunde, and F. Cagnacci. Large herbivore migration plasticity along environmental gradients in Europe: Life-history traits modulate forage effects. *Oikos*, 128(3):416–429, 2019. ISSN 1600-0706. doi: 10.1111/oik.05588.

[44] L. R. Prugh, J. D. Lundquist, B. K. Sullender, C. X. Cunningham, J. Dechow, B. L. Borg, P. J. Sousanes, S. Stehn, and M. T. Durand. Landscape heterogeneity buffers the impact of an extreme weather event on wildlife. *Communications Biology*, 7(1):1–11, Nov. 2024. ISSN 2399-3642. doi: 10.1038/s42003-024-07195-1.

[45] S. Rasmus, J. Räisänen, and M. Lehning. Estimating snow conditions in Finland in the late 21st century using the SNOWPACK model with regional climate scenario data as input. *Annals of Glaciology*, 38:238–244, Jan. 2004. ISSN 0260-3055, 1727-5644. doi: 10.3189/172756404781814843.

[46] S. Rasmus, S. Kivinen, M. Bavay, and J. Heiskanen. Local and regional variability in snow conditions in northern Finland: A reindeer herding perspective. *Ambio*, 45(4): 398–414, May 2016. ISSN 1654-7209. doi: 10.1007/s13280-015-0762-5.

[47] S. Rasmus, T. Horstkotte, M. Turunen, M. Landauer, A. Löf, I. Lehtonen, G. Rosqvist, and Ø. Holand. Reindeer husbandry and climate change: Challenges for adaptation. In *Reindeer Husbandry and Global Environmental Change*. Routledge, 2022.

[48] S. W. Running, R. R. Nemani, and R. D. Hungerford. Extrapolation of synoptic meteorological data in mountainous terrain and its use for simulating forest evapotranspiration and photosynthesis. *Canadian Journal of Forest Research*, 17(6):472–483, June 1987. ISSN 0045-5067. doi: 10.1139/x87-081.

[49] G. Schaefer and R. Paetzold. SNOTEL (SNOwpack TELemetry) and SCAN (soil climate analysis network). Automated weather stations for applications in agriculture and water resources management: Current use and future perspectives, 2000.

[50] D. Scott and D. Kaiser. Variability and trends in united states snowfall over the last half century. Jan. 2004.

[51] W. J. Steenburgh, C. F. Mass, and S. A. Ferguson. The Influence of Terrain-Induced Circulations on Wintertime Temperature and Snow Level in the Washington Cascades. June 1997. ISSN 1520-0434.

[52] C. Stethem and R. Perla. Snow-Slab Studies at Whistler Mountain, British Columbia, Canada. *Journal of Glaciology*, 26(94):85–91, Jan. 1980. ISSN 0022-1430, 1727-5652. doi: 10.3189/S0022143000010613.

[53] I. T. Stewart, D. R. Cayan, and M. D. Dettinger. Changes in Snowmelt Runoff Timing in Western North America under a 'Business as Usual' Climate Change Scenario. *Climatic Change*, 62(1):217–232, Jan. 2004. ISSN 1573-1480. doi: 10.1023/B:CLIM.0000013702.22656.e8.

[54] B. K. Sullender, C. X. Cunningham, J. D. Lundquist, and L. R. Prugh. Defining the danger zone: Critical snow properties for predator–prey interactions. 2023. doi: 10.1111/oik.09925.

[55] D. Vikhamar-Schuler, I. Hanssen-Bauer, T. V. Schuler, S. D. Mathiesen, and M. Lehning. Use of a multilayer snow model to assess grazing conditions for reindeer. *Annals of Glaciology*, 54(62):214–226, Jan. 2013. ISSN 0260-3055, 1727-5644. doi: 10.3189/2013AoG62A306.

[56] J. M. Wallace and P. V. Hobbs. *Atmospheric Science: An Introductory Survey*. Elsevier, Mar. 2006. ISBN 978-0-08-049953-6.

[57] N. E. Wayand, M. P. Clark, and J. D. Lundquist. Diagnosing snow accumulation errors in a rain-snow transitional environment with snow board observations. *Hydrological Processes*, 31(2):349–363, 2017. ISSN 1099-1085. doi: 10.1002/hyp.11002.

[58] N. Wever, S. Würzer, C. Fierz, and M. Lehning. Simulating ice layer formation under the presence of preferential flow in layered snowpacks. *The Cryosphere*, 10(6):2731–2744, Nov. 2016. ISSN 1994-0416. doi: 10.5194/tc-10-2731-2016.